Advances in Nano Research, *Vol. 7 No. 1 (2019) 63-75*
DOI: https://doi.org/10.12989/anr.2019.7.1.063

On static stability of electro-magnetically affected smart magneto-electro-elastic nanoplates

Farzad Ebrahimi * and Mohammad Reza Barati

Mechanical Engineering Department, Faculty of Engineering, Imam Khomeini International University, Qazvin, P.O.B. 16818-34149, Iran

(*Received July 27, 2018, Revised November 20, 2019, Accepted February 15, 2019*)

Abstract. This article represents a quasi-3D theory for the buckling investigation of magneto-electro-elastic functionally graded (MEE-FG) nanoplates. All the effects of shear deformation and thickness stretching are considered within the presented theory. Magneto-electro-elastic material properties are considered to be graded in thickness direction employing power-law distribution. Eringen's nonlocal elasticity theory is exploited to describe the size dependency of such nanoplates. Using Hamilton's principle, the nonlocal governing equations based on quasi-3D plate theory are obtained for the buckling analysis of MEE-FG nanoplates including size effect and they are solved applying analytical solution. It is found that magnetic potential, electric voltage, boundary conditions, nonlocal parameter, power-law index and plate geometrical parameters have significant effects on critical buckling loads of MEE-FG nanoscale plates.

Keywords: magneto-electro-elastic nanoplate; functionally graded material; buckling; Quasi-3D plate theory; nonlocal theory

1. Introduction

An example for a smart material is piezoelectric-magnetic-elastic material in which magnetic-electric environments may lead to mechanical deformation. This means that there is a coupling between magnetic-electric and elastic performances in such materials. In such materials, the material properties can be characterized by elastic, piezoelectric and magnetic constants. Structural components (beams, shells and plates) made of such smart materials are broadly utilized in actuators, sensors and intelligent systems. The material distribution in these structures may be homogenous or non-homogenous. When the material profile is variable thorough the thickness of a structure, the material distribution may be non-homogenous. As an example, a functionally graded material is a non-homogenous material in which two materials are involved and all material properties change from one material to another (Ebrahimi *et al*. 2011, Ebrahimi 2010, Tang *et al*. 2019), Based on the percentage and volume fraction of each material, the complete behavior of the structure can be defined. There are several investigations on smart piezoelectric-magnetic-elastic structures having functionally graded distribution (Pan and Han 2005, Ramirez *et al*. 2006, Wu *et al*. 2010, Tanaka 2018).

The smart material discussed in previous paragraph has been extensively applied in nano-structures and nano-devices. However, at the nanoscale, the behavior of structure differs from macro scale counterpart. This is due to the existence of small size effects (Tounsi *et al*. 2013, Wang *et al*. 2018), Such small size effects are incorporated in non-classical elasticity theories such as Eringen's theory (Eringen 1983) which is also used by other authors (Ke and Wang 2014, Li *et al*. 2014, Ebrahimi and Barati 2016a-d), Functionally graded nanostructures are also studied before based on nonlocal theory introduced by Eringen. The simplest form of this theory involving one scale parameter which defines small scale size-dependency is used in previous researches (Ebrahimi and Dabbagh 2018, Ebrahimi and Barati 2016e-k).

Finally, it can be mentioned that reported papers on buckling of magneto-electro-elastic plates are limited in the literature, especially those at nanoscale. In this article, critical buckling characteristics of MEE-FG nanoplates under magneto-electrical field are examined in the framework of a quasi-3D sinusoidal theory. The present theory accounts for both shear deformation and thickness stretching influences by a higher order variation of displacements through the thickness. Material properties of nanoplate are graded in the thickness direction according to the power-law model. The governing equations are derived by using Hamilton principle and Eringen's nonlocal elasticity theory and are solved via an analytical solution. The detailed mathematical derivations are presented while the emphasis is placed on investigating the effect of several parameters such as external electric voltage, magnetic potential, different boundary conditions, power-law index and nonlocal parameter on buckling characteristics of size-dependent MEE-FG nanoplates.

∗Corresponding author, Ph.D., Professor,
E-mail: febrahimy@ut.ac.ir

http://www.techno-press.org/?journal=journal=anr&subpage=5 ISSN: 2287-237X (Print), 2287-2388 (Online)

2. Governing equations

2.1 Power-law functionally graded material (P-FGM) plate

Each material property (P) for a smart nanoplate shown in Fig. 1 can defined as

$$P = P_2 V_2 + P_1 V_1 \tag{1}$$

P_2 and P_1 are the material properties of top and bottom sides, V_2 and V_1 are the volume fraction of top and bottom surfaces, respectively and are related by

$$V_2 = (\frac{z}{h} + \frac{1}{2})^p, \quad V_1 = 1 - V_2 \tag{2}$$

where ($p \geq 0$) is power-law exponent which determines the material distribution across the plate thickness. Finally, the effective material properties of MEE-FG plates takes the following form

$$P(z) = (P_2 - P_1)\left(\frac{z}{h} + \frac{1}{2}\right)^p + P_1 \tag{3}$$

In this study, the top surface at $z = +h / 2$ of MEE-FG nanoplate is fully $CoFe_2O_4$, whereas the bottom surface ($z = -h / 2$) is fully $BaTio_3$ with the properties presented in Table 1.

2.2 Basic equations

A quasi-3D plate model accounting for shear deformation and thickness stretching effects is considered. The displacement field of present theory can be written as (Hebali *et al*. 2014)

$$u_1(x,y,z) = u(x,y) - z\frac{\partial w_b}{\partial x} - f(z)\frac{\partial w_s}{\partial x} \tag{4}$$

$$u_2(x,y,z) = v(x,y) - z\frac{\partial w_b}{\partial y} - f(z)\frac{\partial w_s}{\partial y} \tag{5}$$

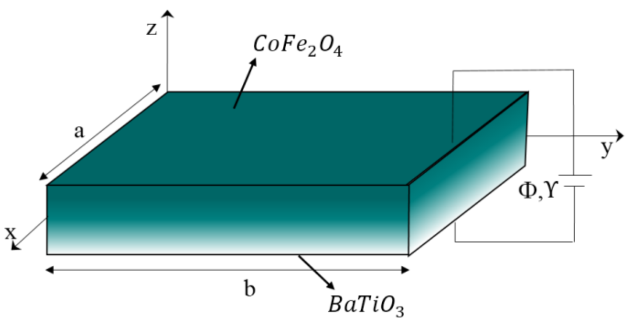

Fig. 1 Geometry of FG nanoplate under magneto-electrical field

Table 1 Magneto-electro-elastic coefficients of material properties (Ramirez *et al*. 2006)

Properties	$BaTiO_3$	$CoFe_2O_4$
$c_{11} = c_{22}$ (GPa)	166	286
c_{33}	162	269.5
$c_{13} = c_{23}$	78	170.5
c_{12}	77	173
c_{55}	43	45.3
c_{66}	44.5	56.5
e_{31} (Cm^{-2})	-4.4	0
e_{33}	18.6	0
e_{15}	11.6	0
q_{31} (N/Am)	0	580.3
q_{33}	0	699.7
q_{15}	0	550
s_{11} (10^{-9} C^2 m^{-2} N^{-1})	11.2	0.08
s_{33}	12.6	0.093
χ_{11} (10^{-6} Ns^2 $C^{-2}/2$)	5	-590
χ_{33}	10	157
$d_{11} = d_{22} = d_{33}$	0	0

$$u_3(x,y,z) = w_b(x,y) + w_s(x,y) + g(z)w_z(x,y) \tag{6}$$

in which u, v, w_b, w_s and w_z are five unknowns of displacements of mid-plane. Also, $f(z)$ is a shape function that determines the distribution of shear stress across the plate thickness. Hence, there is no need for any shear correction factor. The present theory has a function in the form

$$f(z) = z - \sin(\xi z)/\xi \tag{7}$$

The electric potential and magnetic potential distributions across the thickness are approximated via a combination of a cosine and linear variation to satisfy Maxwell's equation in the quasi-static approximation as follows (Ke and Wang 2014)

$$\Phi(x,y,z,t) = -\cos(\xi z)\phi(x,y,t) + \frac{2z}{h}V \tag{8}$$

$$\Upsilon(x,y,z,t) = -\cos(\xi z)\gamma(x,y,t) + \frac{2z}{h}\Omega \tag{9}$$

where $\xi = \pi / h$. Also, V and Ω are the external electric voltage and magnetic potential applied to the MEE-FG plate. Nonzero strains of quasi-3D plate model are expressed by

$$\begin{Bmatrix}\varepsilon_x\\ \varepsilon_y\\ \varepsilon_z\\ \gamma_{xy}\end{Bmatrix} = \begin{Bmatrix}\varepsilon_x^0\\ \varepsilon_y^0\\ g'\varepsilon_z^0\\ \gamma_{xy}^0\end{Bmatrix} + z\begin{Bmatrix}\kappa_x^b\\ \kappa_y^b\\ 0\\ \kappa_{xy}^b\end{Bmatrix} + f\begin{Bmatrix}\kappa_x^s\\ \kappa_y^s\\ 0\\ \kappa_{xy}^s\end{Bmatrix}, \begin{Bmatrix}\gamma_{yz}\\ \gamma_{xz}\end{Bmatrix} = g\begin{Bmatrix}\gamma_{yz}^s\\ \gamma_{xz}^s\end{Bmatrix}, g = 1 - \frac{\partial f}{\partial z} \tag{10}$$

where

$$\begin{Bmatrix} \varepsilon_x^0 \\ \varepsilon_y^0 \\ \varepsilon_z^0 \\ \gamma_{xy}^0 \end{Bmatrix} = \begin{Bmatrix} \frac{\partial u}{\partial x} \\ \frac{\partial v}{\partial y} \\ w_z \\ \frac{\partial u}{\partial y}+\frac{\partial v}{\partial x} \end{Bmatrix}, \begin{Bmatrix} \kappa_x^b \\ \kappa_y^b \\ \kappa_{xy}^b \end{Bmatrix} = \begin{Bmatrix} -\frac{\partial^2 w_b}{\partial x^2} \\ -\frac{\partial^2 w_b}{\partial y^2} \\ -2\frac{\partial^2 w_b}{\partial x \partial y} \end{Bmatrix},$$
$$\begin{Bmatrix} \kappa_x^s \\ \kappa_y^s \\ \kappa_{xy}^s \end{Bmatrix} = \begin{Bmatrix} -\frac{\partial^2 w_s}{\partial x^2} \\ -\frac{\partial^2 w_s}{\partial y^2} \\ -2\frac{\partial^2 w_s}{\partial x \partial y} \end{Bmatrix}, \begin{Bmatrix} \gamma_{yz}^s \\ \gamma_{xz}^s \end{Bmatrix} = \begin{Bmatrix} \frac{\partial w_s}{\partial y}+\frac{\partial w_z}{\partial y} \\ \frac{\partial w_s}{\partial x}+\frac{\partial w_z}{\partial x} \end{Bmatrix} \tag{11}$$

According to Eq. (8), the relation between electric field (E_x, E_y, E_z) and electric potential (Φ), can be obtained as

$$E_x = -\Phi_{,x} = \cos(\xi z)\frac{\partial \phi}{\partial x}, \tag{12}$$

$$E_y = -\Phi_{,y} = \cos(\xi z)\frac{\partial \phi}{\partial y}, \tag{13}$$

$$E_z = -\Phi_{,z} = -\xi \sin(\xi z)\phi - \frac{2V}{h} \tag{14}$$

Also, the relation between magnetic field (H_x, H_y, H_z) and magnetic potential (Υ) can be expressed from Eq. (9) as

$$H_x = -\Upsilon_{,x} = \cos(\xi z)\frac{\partial \gamma}{\partial x}, \tag{15}$$

$$H_y = -\Upsilon_{,y} = \cos(\xi z)\frac{\partial \gamma}{\partial y}, \tag{16}$$

$$H_z = -\Upsilon_{,z} = -\xi \sin(\xi z)\gamma - \frac{2\Omega}{h} \tag{17}$$

Using Hamilton's principle, the equation of motion can be derived by

$$\int_0^t \delta(\Pi_S + \Pi_W)\,dt = 0 \tag{18}$$

Here Π_S is strain energy, Π_W is work done by external forces. The virtual variation of strain energy can be written as

$$\begin{aligned}\delta\Pi_S = \int_v \sigma_{ij}\delta\varepsilon_{ij}\,dV = \int_v (&\sigma_x\delta\varepsilon_x + \sigma_y\delta\varepsilon_y + \sigma_z\delta\varepsilon_z \\ &+\sigma_{xy}\delta\gamma_{xy} + \sigma_{yz}\delta\gamma_{yz} + \sigma_{xz}\delta\gamma_{xz} \\ &-D_x\delta E_x - D_y\delta E_y - D_z\delta E_z \\ &-B_x\delta H_x - B_y\delta H_y - B_z\delta H_z)\,dV\end{aligned} \tag{19}$$

Substituting Eqs. (10) and (11) into Eq. (19) yields

$$\begin{aligned}\delta\Pi_S = \int_0^a\int_0^b [&N_x\frac{\partial\delta u}{\partial x} - M_x^b\frac{\partial^2\delta w_b}{\partial x^2} - M_x^s\frac{\partial^2\delta w_s}{\partial x^2} \\ &+N_y\frac{\partial\delta v}{\partial y} - M_y^b\frac{\partial^2\delta w_b}{\partial y^2} - M_y^s\frac{\partial^2\delta w_s}{\partial y^2} + R_z w_z \\ &+N_{xy}(\frac{\partial\delta u}{\partial y}+\frac{\partial\delta v}{\partial x}) - 2M_{xy}^b\frac{\partial^2\delta w_b}{\partial x\partial y} - 2M_{xy}^s\frac{\partial^2\delta w_s}{\partial x\partial y} \\ &+Q_{yz}(\frac{\partial\delta w_s}{\partial y}+\frac{\partial\delta w_z}{\partial y}) + Q_{xz}(\frac{\partial\delta w_s}{\partial x}+\frac{\partial\delta w_z}{\partial x})]dxdy \\ +\int_0^a\int_0^b\int_{-h/2}^{h/2}[&-D_x\cos(\xi z)\delta\left(\frac{\partial\phi}{\partial x}\right) - D_y\cos(\xi z)\delta\left(\frac{\partial\phi}{\partial y}\right) \\ &+D_z\xi\sin(\xi z)\delta\phi - B_x\cos(\xi z)\delta\left(\frac{\partial\gamma}{\partial x}\right) \\ &-B_y\cos(\xi z)\delta\left(\frac{\partial\gamma}{\partial y}\right) + B_z\xi\sin(\xi z)\delta\gamma]dzdxdy\end{aligned} \tag{20}$$

in which the variables at the last expression are expressed by

$$(N_i, M_i^b, M_i^s) = \int_A (1, z, f)\sigma_i\,dA,\ i = (x, y, xy) \tag{21}$$

$$Q_i = \int_A g\sigma_i\,dA,\ i = (xz, yz) \tag{22}$$

$$R_z = \int_A g'\sigma_z\,dA \tag{23}$$

The first variation of work done by applied forces can be written in the form

$$\begin{aligned}\delta\Pi_W = \int_0^a\int_0^b (&N_x^0\frac{\partial(w_b+w_s+g(z)w_z)}{\partial x}\frac{\partial\delta(w_b+w_s+g(z)w_z)}{\partial x} \\ &+N_y^0\frac{\partial(w_b+w_s+g(z)w_z)}{\partial y}\frac{\partial\delta(w_b+w_s+g(z)w_z)}{\partial y} \\ &+2\delta N_{xy}^0\frac{\partial(w_b+w_s+g(z)w_z)}{\partial x}\frac{\partial(w_b+w_s+g(z)w_z)}{\partial y})dxdy\end{aligned} \tag{24}$$

where N_x^0, N_y^0, N_{xy}^0 are in-plane applied loads. In this study it is assumed that the MEE-FG nanoplate is under external electric voltage, magnetic potential and the shear loading is ignored. So $N_{xy}^0 = 0$ and N_x^0, N_y^0 are the normal forces induced by external electric voltage V and external magnetic potential Ω, respectively and are defined as

$$N_x^0 = N_y^0 = N^b + N^E + N^H \tag{25a}$$

$$N^E = -\int_{-h/2}^{h/2}\tilde{e}_{31}\frac{2V}{h}dz,\ N^H = -\int_{-h/2}^{h/2}\tilde{q}_{31}\frac{2\Omega}{h}dz \tag{25b}$$

The equations of motion for a quasi-3D MEE-FG nanoplate are obtained by inserting Eqs. (20) and (24) in Eq. (18) when the coefficients of δu, δv, δw_b, δw_s, δw_z, $\delta\phi$ and $\delta\gamma$ are equal to zero

$$\frac{\partial N_x}{\partial x}+\frac{\partial N_{xy}}{\partial y}=0 \tag{26}$$

$$\frac{\partial N_x}{\partial x}+\frac{\partial N_{xy}}{\partial y}=0 \tag{27}$$

$$\begin{aligned}&\frac{\partial^2 M_x^b}{\partial x^2}+2\frac{\partial^2 M_{xy}^b}{\partial x\partial y}+\frac{\partial^2 M_y^b}{\partial y^2}\\&-(N^b+N^E+N^H)\nabla^2(w_b+w_s+gw_z)=0\end{aligned} \tag{28}$$

$$\begin{aligned}&\frac{\partial^2 M_x^s}{\partial x^2}+2\frac{\partial^2 M_{xy}^s}{\partial x\partial y}+\frac{\partial^2 M_y^s}{\partial y^2}+\frac{\partial Q_{xz}}{\partial x}+\frac{\partial Q_{yz}}{\partial y}\\&-(N^b+N^E+N^H)\nabla^2(w_b+w_s+gw_z)=0\end{aligned} \tag{29}$$

$$\begin{aligned}&\frac{\partial Q_{xz}}{\partial x}+\frac{\partial Q_{yz}}{\partial y}-R_z\\&-g(N^b+N^E+N^H)\nabla^2(w_b+w_s+gw_z)=0\end{aligned} \tag{30}$$

$$\begin{aligned}\int_{-h/2}^{h/2}\Bigg(&\cos(\xi z)\frac{\partial D_x}{\partial x}+\cos(\xi z)\frac{\partial D_y}{\partial y}\\&+\xi\sin(\xi z)D_z\Bigg)dz=0\end{aligned} \tag{31}$$

$$\int_{-h/2}^{h/2}\left(\cos(\xi z)\frac{\partial B_x}{\partial x}+\cos(\xi z)\frac{\partial B_y}{\partial y}+\xi\sin(\xi z)B_z\right)dz=0 \tag{32}$$

2.3 Nonlocal elasticity theory for the magneto-electro-elastic materials

In general form, the nonlocal elasticity for smart piezo-magnetic-elastic materials can be defined as

$$\begin{aligned}\sigma_{ij}=\int_V\alpha\left(|x'-x|,\tau\right)\big[&C_{ijkl}\varepsilon_{kl}(x')\\&-e_{mij}E_m(x')-q_{nij}H_n(x')\big]dV(x')\end{aligned} \tag{33a}$$

$$\begin{aligned}D_i=\int_V\alpha\left(|x'-x|,\tau\right)\big[&e_{ikl}\varepsilon_{kl}(x')\\&+s_{im}E_m(x')+d_{in}H_n(x')\big]dV(x')\end{aligned} \tag{33b}$$

$$\begin{aligned}B_i=\int_V\alpha\left(|x'-x|,\tau\right)\big[&q_{ikl}\varepsilon_{kl}(x')\\&+d_{im}E_m(x')+\chi_{in}H_n(x')\big]dV(x')\end{aligned} \tag{33c}$$

in which σ_{ij}, D_i, B_i denotes the components of stress, electric displacement and magnetic induction. Also, all of other parameters are completely defined and discussed in previous papers (Ke and Wang 2014, Ebrahimi and Barati 2016b), The differential form of nonlocal elasticity with one scale parameter e_0a can be represented as

$$\sigma_{ij}-(e_0a)^2\nabla^2\sigma_{ij}=C_{ijkl}\varepsilon_{kl}-e_{mij}E_m-q_{nij}H_n \tag{34a}$$

$$D_i-(e_0a)^2\nabla^2 D_i=e_{ikl}\varepsilon_{kl}+s_{im}E_m+d_{in}H_n \tag{34b}$$

$$B_i-(e_0a)^2\nabla^2 B_i=q_{ikl}\varepsilon_{kl}+d_{im}E_m+\chi_{in}H_n \tag{34c}$$

where ∇^2 is the Laplacian operator. The constitutive equations can be expressed by

$$(1-\mu\nabla^2)\sigma_{xx}=\tilde{C}_{11}\varepsilon_{xx}+\tilde{C}_{12}\varepsilon_{yy}+\tilde{C}_{13}\varepsilon_{zz}-\tilde{e}_{31}E_z-\tilde{q}_{31}H_z \tag{35}$$

$$(1-\mu\nabla^2)\sigma_{yy}=\tilde{C}_{12}\varepsilon_{xx}+\tilde{C}_{11}\varepsilon_{yy}+\tilde{C}_{13}\varepsilon_{zz}-\tilde{e}_{31}E_z-\tilde{q}_{31}H_z \tag{36}$$

$$(1-\mu\nabla^2)\sigma_{zz}=\tilde{C}_{13}\varepsilon_{xx}+\tilde{C}_{13}\varepsilon_{yy}+\tilde{C}_{33}\varepsilon_{zz}-\tilde{e}_{33}E_z-\tilde{q}_{33}H_z \tag{37}$$

$$(1-\mu\nabla^2)\sigma_{xy}=\tilde{C}_{66}\gamma_{xy} \tag{38}$$

$$(1-\mu\nabla^2)\sigma_{xz}=\tilde{C}_{55}\gamma_{xz}-\tilde{e}_{15}E_x-\tilde{q}_{15}H_x \tag{39}$$

$$(1-\mu\nabla^2)\sigma_{yz}=\tilde{C}_{55}\gamma_{yz}-\tilde{e}_{15}E_y-\tilde{q}_{15}H_y \tag{40}$$

$$(1-\mu\nabla^2)D_x=\tilde{e}_{15}\gamma_{xz}+\tilde{s}_{11}E_x+\tilde{d}_{11}H_x \tag{41}$$

$$(1-\mu\nabla^2)D_y=\tilde{e}_{15}\gamma_{yz}+\tilde{s}_{11}E_y+\tilde{d}_{11}H_y \tag{42}$$

$$(1-\mu\nabla^2)D_z=\tilde{e}_{31}\varepsilon_{xx}+\tilde{e}_{31}\varepsilon_{yy}+\tilde{e}_{33}\varepsilon_{zz}+\tilde{s}_{33}E_z+\tilde{d}_{33}H_z \tag{43}$$

$$(1-\mu\nabla^2)B_x=\tilde{q}_{15}\gamma_{xz}+\tilde{d}_{11}E_x+\tilde{\chi}_{11}H_x \tag{44}$$

$$(1-\mu\nabla^2)B_y=\tilde{q}_{15}\gamma_{yz}+\tilde{d}_{11}E_y+\tilde{\chi}_{11}H_y \tag{45}$$

$$(1-\mu\nabla^2)B_z=\tilde{q}_{31}\varepsilon_{xx}+\tilde{q}_{31}\varepsilon_{yy}+\tilde{q}_{33}\varepsilon_{zz}+\tilde{d}_{33}E_z+\tilde{\chi}_{33}H_z \tag{46}$$

where $\tilde{C}_{ij},\tilde{e}_{ij},\tilde{q}_{ij},\tilde{d}_{ij},\tilde{s}_{ij}$ and $\tilde{\chi}_{ij}$ are reduced constants for the FG plate under the plane stress state (Ke and Wang 2014) which are given as

$$\begin{aligned}&\tilde{C}_{11}=C_{11}-\frac{C_{13}^2}{C_{33}},\ \tilde{C}_{12}=C_{12}-\frac{C_{13}^2}{C_{33}},\ \tilde{C}_{66}=C_{66},\\&\tilde{e}_{15}=e_{15},\quad \tilde{e}_{31}=e_{31}-\frac{C_{13}e_{33}}{c_{33}},\\&\tilde{q}_{15}=q_{15},\ \tilde{q}_{31}=q_{31}-\frac{C_{13}q_{33}}{C_{33}},\\&\tilde{d}_{11}=\tilde{d}_{11},\quad \tilde{d}_{33}=\tilde{d}_{33}+\frac{q_{33}e_{33}}{C_{33}},\\&\tilde{s}_{11}=s_{11},\quad \tilde{s}_{33}=s_{33}+\frac{e_{33}^2}{C_{33}},\\&\tilde{\chi}_{11}=\chi_{11},\quad \tilde{\chi}_{33}=\chi_{33}+\frac{q_{33}^2}{C_{33}}\end{aligned} \tag{47}$$

By integrating Eqs. (35)-(46) over the area of plate cross-section, the complete relations for the force-strain and the moment-strain and other necessary relation of the presented can be obtained. The governing equations of quasi-3D MEE-FG nanoplate in terms of the displacements and potentials can be derived by substituting Eqs. (A1)-(A9), into Eqs. (26)-(32) as follows

$$\begin{aligned}&A_{11}\frac{\partial^2 u}{\partial x^2}+A_{66}\frac{\partial^2 u}{\partial y^2}+(A_{12}+A_{66})\frac{\partial^2 v}{\partial x\partial y}\\&-B_{11}\frac{\partial^3 w_b}{\partial x^3}-(B_{12}+2B_{66})\frac{\partial^3 w_b}{\partial x\partial y^2}-B_{11}^s\frac{\partial^3 w_s}{\partial x^3}\\&-(B_{12}^s+2B_{66}^s)\frac{\partial^3 w_s}{\partial x\partial y^2}+A_{31}^e\frac{\partial \phi}{\partial x}+A_{31}^m\frac{\partial \gamma}{\partial x}+X_{13}\frac{\partial w_z}{\partial x}=0\end{aligned}\tag{48}$$

$$\begin{aligned}&A_{66}\frac{\partial^2 v}{\partial x^2}+A_{22}\frac{\partial^2 v}{\partial y^2}+(A_{12}+A_{66})\frac{\partial^2 u}{\partial x\partial y}\\&-B_{22}\frac{\partial^3 w_b}{\partial y^3}-(B_{12}+2B_{66})\frac{\partial^3 w_b}{\partial x^2\partial y}-B_{22}^s\frac{\partial^3 w_s}{\partial y^3}\\&-(B_{12}^s+2B_{66}^s)\frac{\partial^3 w_s}{\partial x^2\partial y}+A_{31}^e\frac{\partial \phi}{\partial y}+A_{31}^m\frac{\partial \gamma}{\partial y}+X_{13}\frac{\partial w_z}{\partial y}=0\end{aligned}\tag{49}$$

$$\begin{aligned}&B_{11}\frac{\partial^3 u}{\partial x^3}+(B_{12}+2B_{66})\frac{\partial^3 u}{\partial x\partial y^2}+(B_{12}+2B_{66})\frac{\partial^3 v}{\partial x^2\partial y}\\&+B_{22}\frac{\partial^3 v}{\partial y^3}-D_{11}\frac{\partial^4 w_b}{\partial x^4}+E_{31}^e(\frac{\partial^2\phi}{\partial x^2}+\frac{\partial^2\phi}{\partial y^2})\\&-A_{15}^e(\frac{\partial^2\phi}{\partial x^2}+\frac{\partial^2\phi}{\partial y^2})-2(D_{12}+2D_{66})\frac{\partial^4 w_b}{\partial x^2\partial y^2}\\&-D_{22}\frac{\partial^4 w_b}{\partial y^4}-D_{11}^s\frac{\partial^4 w_s}{\partial x^4}\\&-2(D_{12}^s+2D_{66}^s)\frac{\partial^4 w_s}{\partial x^2\partial y^2}\\&+E_{31}^m(\frac{\partial^2\gamma}{\partial x^2}+\frac{\partial^2\gamma}{\partial y^2})-A_{15}^e(\frac{\partial^2\gamma}{\partial x^2}+\frac{\partial^2\gamma}{\partial y^2})\\&-D_{22}^s\frac{\partial^4 w_s}{\partial y^4}+Y_{13}(\frac{\partial^2 w_z}{\partial x^2}+\frac{\partial^2 w_z}{\partial y^2})\\&+(1-\mu\nabla^2)(-(N^b+N^E+N^H)\\&\nabla^2(w_b+w_s+gw_z))=0\end{aligned}\tag{50}$$

$$\begin{aligned}&B_{11}^s\frac{\partial^3 u}{\partial x^3}+(B_{12}^s+2B_{66}^s)\frac{\partial^3 u}{\partial x\partial y^2}\\&+(B_{12}^s+2B_{66}^s)\frac{\partial^3 v}{\partial x^2\partial y}+B_{22}^s\frac{\partial^3 v}{\partial y^3}\\&-D_{11}^s\frac{\partial^4 w_b}{\partial x^4}-A_{15}^e(\frac{\partial^2\phi}{\partial x^2}+\frac{\partial^2\phi}{\partial y^2})\\&+A_{55}^s\frac{\partial^2 w_s}{\partial x^2}+A_{44}^s\frac{\partial^2 w_s}{\partial y^2}\\&-2(D_{12}^s+2D_{66}^s)\frac{\partial^4 w_b}{\partial x^2\partial y^2}-D_{22}^s\frac{\partial^4 w_b}{\partial y^4}\\&-H_{11}^s\frac{\partial^4 w_s}{\partial x^4}-2(H_{12}^s+2H_{66}^s)\frac{\partial^4 w_s}{\partial x^2\partial y^2}\\&-H_{22}^s\frac{\partial^4 w_s}{\partial y^4}+F_{31}^e(\frac{\partial^2\phi}{\partial x^2}+\frac{\partial^2\phi}{\partial y^2})\\&+F_{31}^m(\frac{\partial^2\gamma}{\partial x^2}+\frac{\partial^2\gamma}{\partial y^2})-A_{15}^m(\frac{\partial^2\gamma}{\partial x^2}+\frac{\partial^2\gamma}{\partial y^2})\\&+(A_{55}^s+Y_{13}^s)\frac{\partial^2 w_z}{\partial x^2}+(A_{44}^s+Y_{23}^s)\frac{\partial^2 w_z}{\partial y^2}\\&+(1-\mu\nabla^2)(-(N^b+N^E+N^H)\\&\nabla^2(w_b+w_s+gw_z))=0\end{aligned}\tag{51}$$

$$\begin{aligned}&-X_{13}(\frac{\partial u}{\partial x}+\frac{\partial v}{\partial y})+Y_{13}(\frac{\partial^2 w_b}{\partial x^2}+\frac{\partial^2 w_b}{\partial y^2})\\&+Y_{13}^s(\frac{\partial^2 w_s}{\partial x^2}+\frac{\partial^2 w_s}{\partial y^2})+A_{44}^s(\frac{\partial^2 w_s}{\partial y^2}+\frac{\partial^2 w_z}{\partial y^2})\\&+A_{55}^s(\frac{\partial^2 w_s}{\partial x^2}+\frac{\partial^2 w_z}{\partial x^2})\\&-Z_{33}w_z-H_{33}^e\phi-H_{33}^m\gamma+g(1-\mu\nabla^2)\\&\nabla^2(w_b+w_s+gw_z))=0\end{aligned}\tag{52}$$

$$\begin{aligned}&A_{31}^e(\frac{\partial u}{\partial x}+\frac{\partial v}{\partial y})-E_{31}^e(\frac{\partial^2 w_b}{\partial x^2}+\frac{\partial^2 w_b}{\partial y^2})\\&-(F_{31}^e-E_{15}^e)(\frac{\partial^2 w_s}{\partial x^2}+\frac{\partial^2 w_s}{\partial y^2})+F_{11}^e(\frac{\partial^2\phi}{\partial x^2}+\frac{\partial^2\phi}{\partial y^2})\\&+F_{11}^m(\frac{\partial^2\gamma}{\partial x^2}+\frac{\partial^2\gamma}{\partial y^2})+H_{33}^e w_z-F_{33}^e\phi-F_{33}^m\gamma=0\end{aligned}\tag{53}$$

$$\begin{aligned}&A_{31}^m(\frac{\partial u}{\partial x}+\frac{\partial v}{\partial y})-E_{31}^m(\frac{\partial^2 w_b}{\partial x^2}+\frac{\partial^2 w_b}{\partial y^2})\\&-(F_{31}^m-E_{15}^m)(\frac{\partial^2 w_s}{\partial x^2}+\frac{\partial^2 w_s}{\partial y^2})+F_{11}^m(\frac{\partial^2\phi}{\partial x^2}+\frac{\partial^2\phi}{\partial y^2})\\&+X_{11}^m(\frac{\partial^2\gamma}{\partial x^2}+\frac{\partial^2\gamma}{\partial y^2})+H_{33}^m w_z-F_{33}^m\phi-X_{33}^m\gamma=0\end{aligned}\tag{54}$$

3. Solution procedure

Based on Galerkin's method, it is possible to provide a solution for buckling problem of quasi-3D piezo-magnetic nanoplates based on the boundary conditions:

- Simply-supported (S)

$$\begin{aligned}&w_b=w_s=N_x=M_x=0 \quad \text{at} \quad x=0,\,a\\&w_b=w_s=N_y=M_y=0 \quad \text{at} \quad y=0,\,b\end{aligned}\tag{55}$$

- Clamped (C)

$$u=v=w_b=w_s=0 \quad \text{at} \quad x=0,\,a \quad \text{and} \quad y=0,\,b\tag{56}$$

- Free (F)

$$\begin{aligned}&M_x=M_{xy}=Q_{xz}=0 \quad \text{at} \quad x=0,\ a\\&M_y=M_{xy}=Q_{yz}=0 \quad \text{at} \quad y=0,\ b\end{aligned}\tag{57}$$

In next step, the seven variables based on quasi-3D piezo-magnetic plate model can be defined by

$$u=\sum_{m=1}^{\infty}\sum_{n=1}^{\infty}U_{mn}\frac{\partial X_m(x)}{\partial x}Y_n(y) \tag{58}$$

$$v=\sum_{m=1}^{\infty}\sum_{n=1}^{\infty}V_{mn}X_m(x)\frac{\partial Y_n(y)}{\partial y} \tag{59}$$

$$w_b=\sum_{m=1}^{\infty}\sum_{n=1}^{\infty}W_{bmn}X_m(x)Y_n(y) \tag{60}$$

$$w_s=\sum_{m=1}^{\infty}\sum_{n=1}^{\infty}W_{smn}X_m(x)Y_n(y) \tag{61}$$

$$w_z=\sum_{m=1}^{\infty}\sum_{n=1}^{\infty}W_{zmn}X_m(x)Y_n(y) \tag{62}$$

$$\phi=\sum_{m=1}^{\infty}\sum_{n=1}^{\infty}\Phi_{mn}X_m(x)Y_n(y) \tag{63}$$

$$\gamma=\sum_{m=1}^{\infty}\sum_{n=1}^{\infty}\Upsilon_{mn}X_m(x)Y_n(y) \tag{64}$$

where (U_{mn}, V_{mn}, W_{bmn}, W_{smn}, W_{zmn}, Φ_{mn}, γ_{mn}) are the unknown coefficients and the functions X_m and Y_n are tabulated in detail in Table 2 for different boundary conditions ($\alpha = m\pi / a$, $\beta = m\pi / b$), Inserting Eqs. (58)-(64) into Eqs. (48)-(54) respectively, leads to

$$\begin{aligned}&[(A_{11}r_1+A_{66}r_2)]U_{mn}+(A_{12}+A_{66})r_2V_{mn}\\&-[B_{11}r_1+(B_{12}+2B_{66})r_2]W_{bmn}+[-(B^s_{12}+2B^s_{66})r_2\\&-B^s_{11}r_1)]W_{smn}+A^e_{31}r_{11}\Phi_{mn}+A^m_{31}r_{11}\Upsilon_{mn}+X_{13}r_{11}W_{zmn}=0\end{aligned} \tag{65}$$

$$\begin{aligned}&[(A_{12}+A_{66})r_3]U_{mn}+[A_{66}r_3+A_{22}r_4]V_{mn}\\&-(B_{12}+2B_{66})r_3]W_{bmn}+[-B^s_{22}r_4-(B^s_{12}+2B^s_{66})r_1]W_{smn}\\&+A^e_{31}r_{12}\Phi_{mn}+A^m_{31}r_{12}\Upsilon_{mn}+X_{13}r_{12}W_{zmn}=0\end{aligned} \tag{66}$$

$$\begin{aligned}&[B_{11}r_5+(B_{12}+2B_{66})r_6]U_{mn}+[(B_{12}+2B_{66})r_6+B_{22}r_7]V_{mn}\\&+[-D_{11}r_5-2(D_{12}+2D_{66})r_6-D_{22}r_7)\\&+(N^b+N^E+N^H)(\mu(r_5+2r_6+r_7)-(r_{10}+r_9))]W_{bmn}\\&+[-D^s_{11}r_5-2(D^s_{12}+2D^s_{66})r_6-D^s_{22}r_7\\&+(N^b+N^E+N^H)(\mu(r_5+2r_6+r_7)\\&-(r_{10}+r_9))]W_{smn}+[E^e_{31}(r_{10}+r_9)]\Phi_{mn}+[E^m_{31}(r_9+r_{10})]\Upsilon_{mn}\\&+[Y_{13}(r_9+r_{10})+g(N^b+N^E+N^H)\\&(\mu(r_5+2r_6+r_7)-(r_{10}+r_9))]W_{zmn}=0\end{aligned} \tag{67}$$

$$\begin{aligned}&[B^s_{11}r_5+(B^s_{12}+2B^s_{66})r_6]U_{mn}+[(B^s_{12}+2B^s_{66})r_6+B^s_{22}r_7]V_{mn}\\&+[-D^s_{11}r_5-2(D^s_{12}+2D^s_{66})r_6-D^s_{22}r_7)\\&+(N^b+N^E+N^H)(\mu(r_5+2r_6+r_7)-(r_{10}+r_9))]W_{bmn}\\&+[A^s_{44}(r_{10}+r_9)-H^s_{11}r_5-2(H^s_{12}+2H^s_{66})r_6-H^s_{22}r_7\\&+(N^b+N^E+N^H)(\mu(r_5+2r_6+r_7)-(r_{10}+r_9))\end{aligned} \tag{68}$$

$$\begin{aligned}&-\mu(r_5+2r_6+r_7))]W_{smn}+[(F^e_{31}-A^e_{15})(r_{10}+r_9)]\Phi_{mn}\\&+(F^m_{31}-A^m_{15})(r_{10}+r_9)\Upsilon_{mn}+[(Y^s_{13}+A^s_{44})(r_9+r_{10})\\&+g(N^b+N^E+N^H)(\mu(r_5+2r_6+r_7)\\&-(r_{10}+r_9))]W_{zmn}=0\end{aligned} \tag{68}$$

$$\begin{aligned}&[-X_{13}r_{10}]U_{mn}+[-X_{13}r_9]V_{mn}+[Y_{13}(r_9+r_{10})\\&+g(N^b+N^E+N^H)(\mu(r_5+2r_6+r_7)\\&-(r_{10}+r_9))]]W_{bmn}+[(Y^s_{13}+A^s_{44})(r_9+r_{10})\\&+g(N^b+N^E+N^H)(\mu(r_5+2r_6+r_7)\\&-(r_{10}+r_9))]]W_{smn}+[-Z_{33}r_8\\&+g^2(N^b+N^E+N^H)(\mu(r_5+2r_6+r_7)\\&-(r_{10}+r_9))]W_{zmn}+H^e_{33}r_8\Phi_{mn}+H^m_{33}r_8\Upsilon_{mn}=0\end{aligned} \tag{69}$$

$$\begin{aligned}&A^e_{31}r_{10}U_{mn}+A^e_{31}r_9V_{mn}+[-E^e_{31}(r_{10}+r_9)]W_{bmn}\\&+[(E^e_{15}-F^e_{31})(r_{10}+r_9)]W_{smn}+[F^e_{11}(r_{10}+r_9)-F^e_{33}r_8]\Phi_{mn}\\&+[F^m_{11}(r_{10}+r_9)-F^m_{33}r_8]\Upsilon_{mn}+H^e_{33}r_8W_{zmn}=0\end{aligned} \tag{70}$$

$$\begin{aligned}&A^m_{31}r_{10}U_{mn}+A^m_{31}r_9V_{mn}-E^m_{31}(r_{10}+r_9)W_{bmn}\\&+(E^m_{15}-F^m_{31})(r_{10}+r_9)W_{smn}+[F^m_{11}(r_{10}+r_9)-F^m_{33}r_8]\Phi_{mn}\\&+[X^m_{11}(r_{10}+r_9)-X^m_{33}r_8]\Upsilon_{mn}+H^m_{33}r_8W_{zmn}=0\end{aligned} \tag{71}$$

where

$$\begin{aligned}\{r_3,r_4,r_{12}\}=\int_0^a\int_0^b X(x)Y'(y)\{X''(x)Y'(y),\\X(x)Y'''(y),X(x)Y'(y)\}dxdy\end{aligned} \tag{72}$$

$$\begin{aligned}\{r_1,r_2,r_{11}\}=\int_0^a\int_0^b X'(x)Y(y)\{X'''(x)Y(y),\\X'(x)Y''(y),X'(x)Y(y)\}dxdy\end{aligned} \tag{73}$$

$$\begin{aligned}\{r_5,r_6,r_7\}=\int_0^a\int_0^b X(x)Y(y)\{X''''(x)Y(y),\\X''(x)Y''(y),X(x)Y''''(y)\}dxdy\end{aligned} \tag{74}$$

$$\begin{aligned}\{r_8,r_9,r_{10}\}=\int_0^a\int_0^b X(x)Y(y)\{X(x)Y(y),\\X(x)Y''(y),X''(x)Y(y)\}dxdy\end{aligned} \tag{75}$$

By finding the coefficient of stiffness matrix from above equations, one can write

$$[K]_{7*7}\begin{bmatrix}U_{mn}\\V_{mn}\\W_{bmn}\\W_{smn}\\W_{zmn}\\\Psi_{mn}\\\Upsilon_{mn}\end{bmatrix}=0 \tag{76}$$

The non-trivial solution is obtained when the determinant of stiffness matrix is set to zero ($|K| = 0$) to find critical buckling loads. The non-dimensional form of buckling load can be defined by

$$\bar{N} = N^b \frac{a^2}{D_c}, \; D_c = c_{11}^u h^3 \tag{77}$$

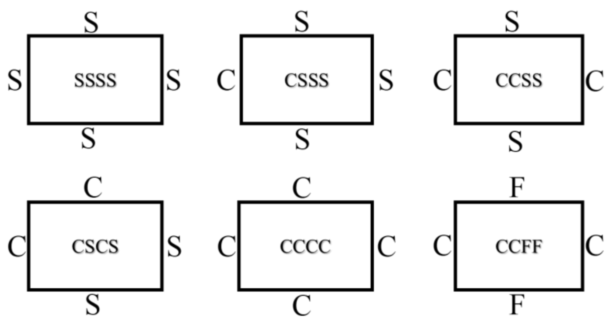

Fig. 2 Boundary conditions of FG nanoplate

4. Numerical results and discussions

In this section, effects of different parameters such as magneto-electrical field, nonlocality, boundary conditions and material composition on critical buckling loads of MEE-FG nanoplates are examined. Considered boundary conditions for nanoplate are illustrated in Fig. 2. The length of nanoplate is considered to be a = 10 nm. For the verification purpose, critical buckling loads are campared with those of FG nanoplates presented by Sobhy (2015) and a good agreement is found according to the results presented in Table 3. For the verification study, the material properties are assumed as: Ec = 380 GPa, Em = 70 GPa and vc = vm = 0.3.

In Figs. 3 and 4, variation of dimensionless buckling load of MEE-FG nanoplates vesus power-law index (p) is illustrated for different boundary conditions, electric voltages and magnetic potentials when a/h = 100 and μ = 0.5 nm^2. It is deduced that critical buckling loads of MEE-FG nanoplate are siginificantely influenced by the magnitude and sign of magnetic and electric potentials for every value of power-law index. It is concluded that negative values of magnetic potential give lower buckling loads than positive magnetic potentials for all boundary conditions. While, smaller values of electric voltage lead to

Table 2 The admissible functions $X_m(x)$ and $Y_n(y)$

	Boundary conditions		The functions X_m and Y_n	
	At x = 0, a	At y = 0, b	$X_m(x)$	$Y_n(y)$
SSSS	$X_m(0) = X_m''(0) = 0$ $X_m(a) = X_m''(a) = 0$	$Y_n(0) = Y_n''(0) = 0$ $Y_n(b) = Y_n''(b) = 0$	$Sin(\alpha x)$	$Sin(\beta y)$
CSSS	$X_m(0) = X_m'(0) = 0$ $X_m(a) = X_m''(a) = 0$	$Y_n(0) = Y_n''(0) = 0$ $Y_n(b) = Y_n''(b) = 0$	$Sin(\alpha x)[Cos(\alpha x) - 1]$	$Sin(\beta y)$
CSCS	$X_m(0) = X_m'(0) = 0$ $X_m(a) = X_m''(a) = 0$	$Y_n(0) = Y_n'(0) = 0$ $Y_n(b) = Y_n''(b) = 0$	$Sin(\alpha x)[Cos(\alpha x) - 1]$	$Sin(\beta y)[Cos(\beta y) - 1]$
CCSS	$X_m(0) = X_m'(0) = 0$ $X_m(a) = X_m'(a) = 0$	$Y_n(0) = Y_n''(0) = 0$ $Y_n(b) = Y_n''(b) = 0$	$Sin^2(\alpha x)$	$Sin(\beta y)$
CCCC	$X_m(0) = X_m'(0) = 0$ $X_m(a) = X_m'(a) = 0$	$Y_n(0) = Y_n'(0) = 0$ $Y_n(b) = Y_n'(b) = 0$	$Sin^2(\alpha x)$	$Sin^2(\beta y)$
CCFF	$X_m''(0) = X_m'''(0) = 0$ $X_m''(a) = X_m'''(a) = 0$	$Y_n(0) = Y_n'(0) = 0$ $Y_n(b) = Y_n'(b) = 0$	$Sin^2(\alpha x)$	$Cos^2(\beta y)[Sin^2(\beta y) + 1]$

Table 3 Comparison of critical buckling load of simply-supported FG nanoplates (a/b = 1, a/h = 10)

	μ = 0 nm^2		μ = 2 nm^2	
Gradient index, p	(Sobhy 2015)	Present	(Sobhy 2015)	Present
0	18.6876	18.6877	10.4425	10.4426
0.5	10.0638	10.0638	5.6235	5.62359
2.5	6.2593	6.25935	3.4976	3.49769
5.5	5.5200	5.52002	3.0845	3.08455
10.5	4.9677	4.96776	2.7759	2.77596

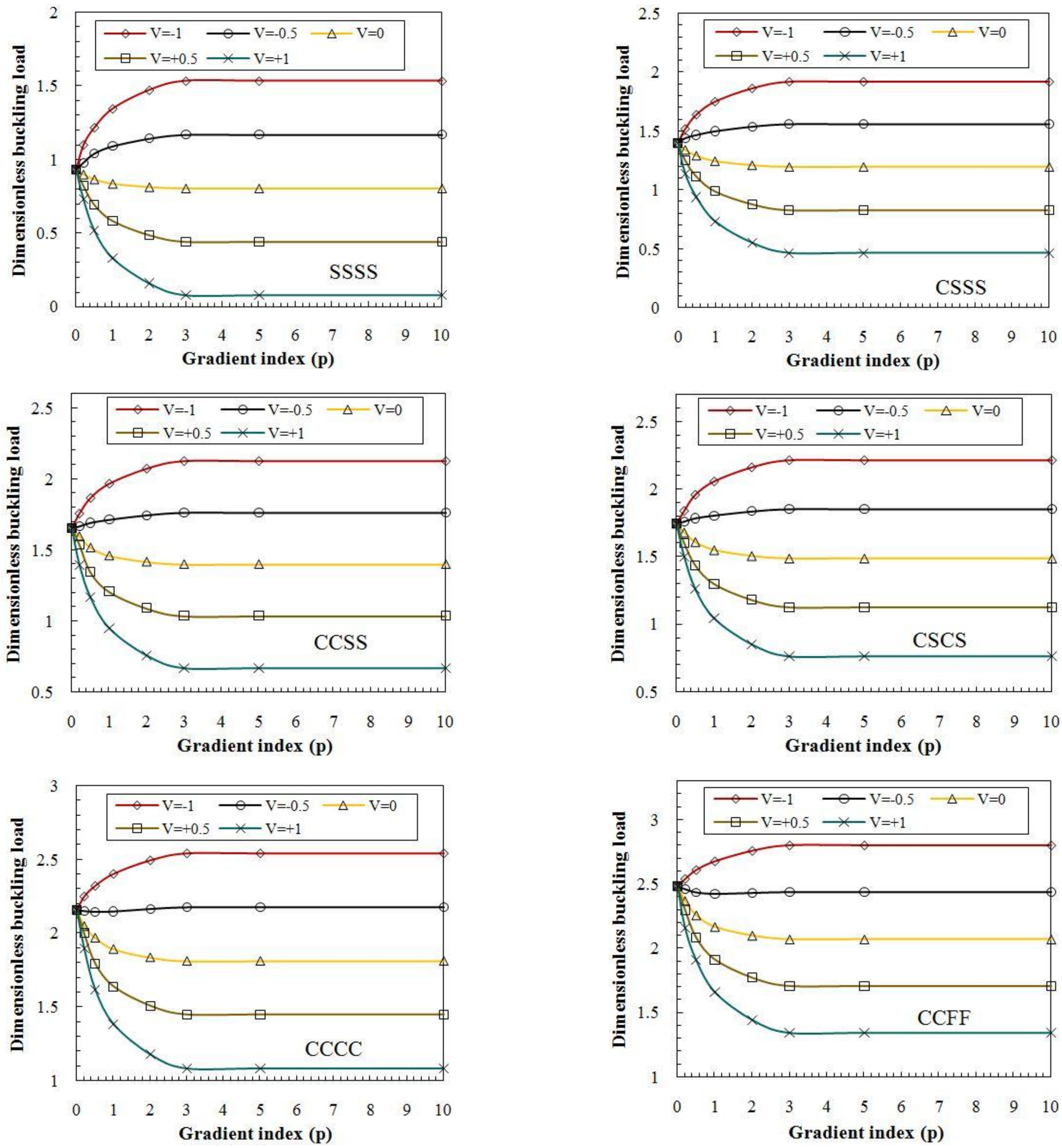

Fig. 3 Buckling load curves of the nanoplate versus gradient index for different electric voltages (a/h = 100, μ = 0.5 nm^2, $\Omega = 0\times 10^{-5}$)

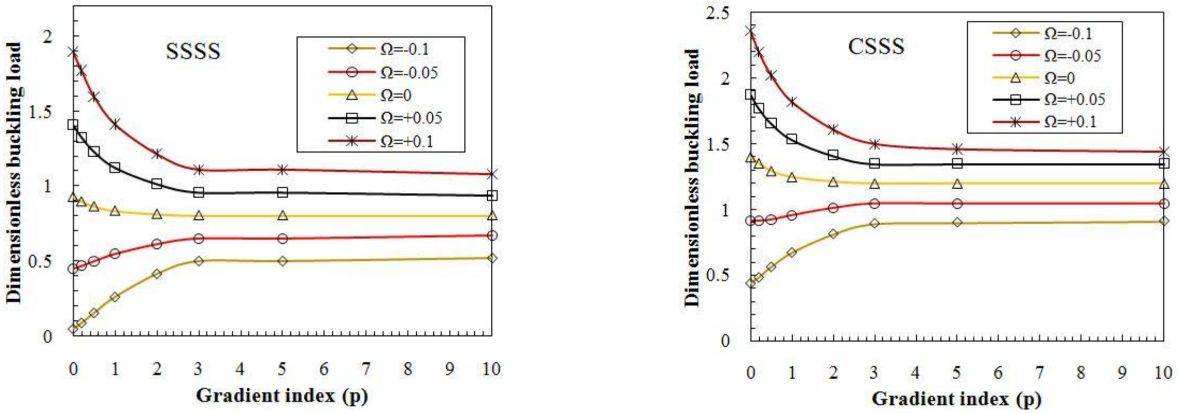

Fig. 4 Buckling load curves of the nanoplate versus gradient index for various magnetic potentials (a/h = 100, μ = 0.5 nm^2, $V = 0\times 10^{-4}$)

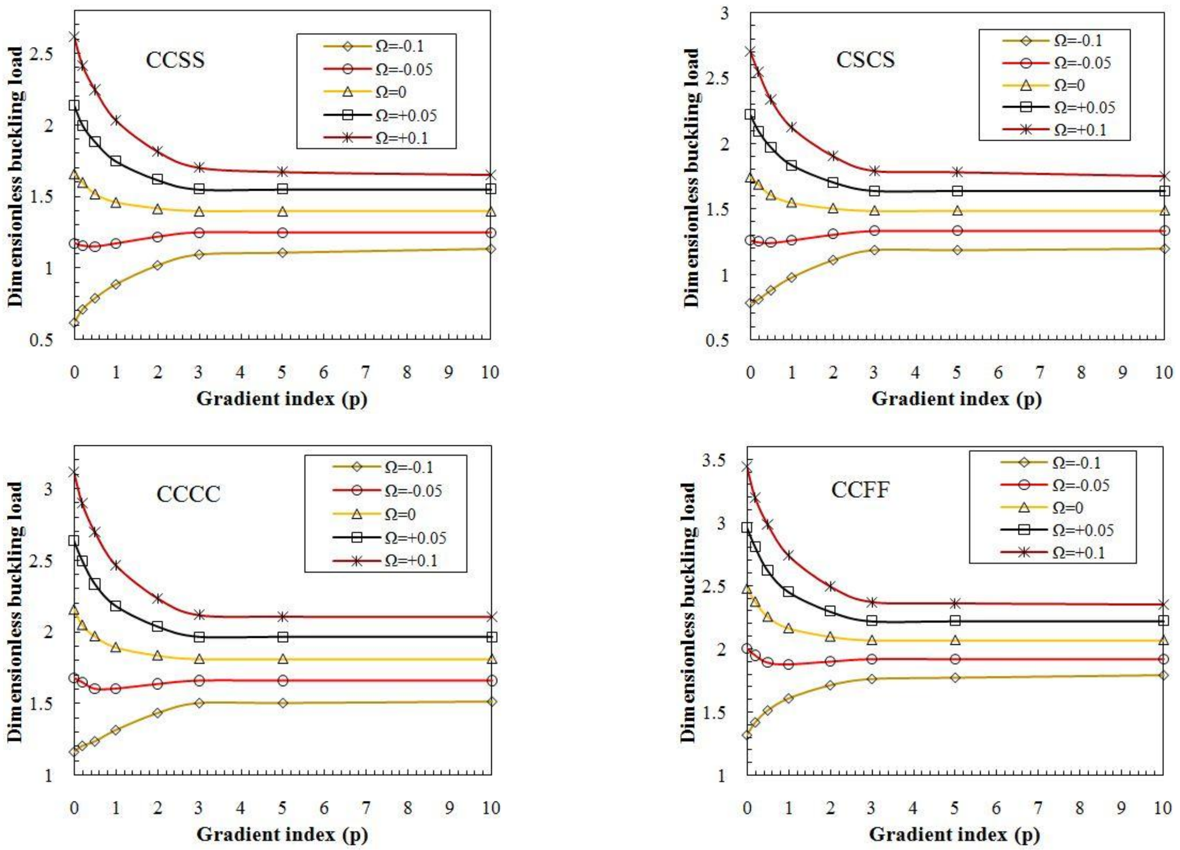

Fig. 4 Continued

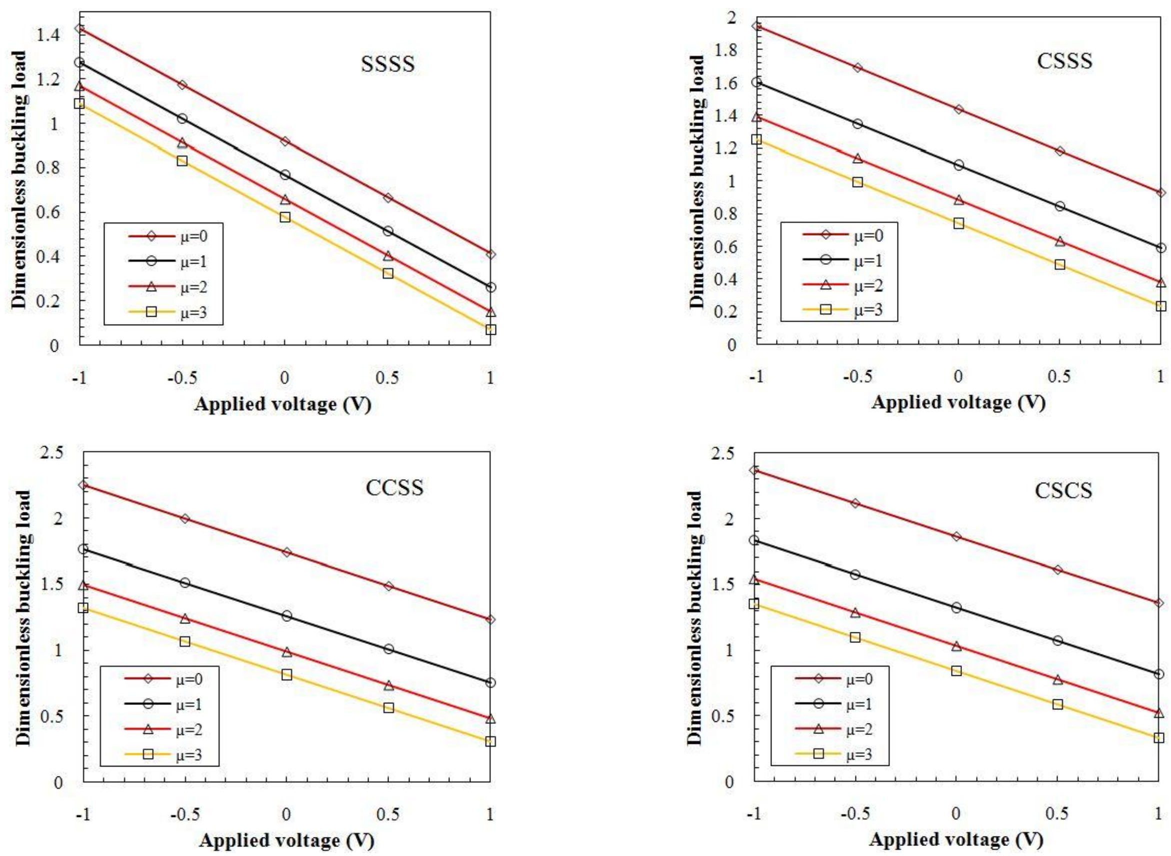

Fig. 5 Buckling load curves of the nanoplate versus applied voltage for various nonlocal parameters (a/h = 100, p = 1, Ω = 0)

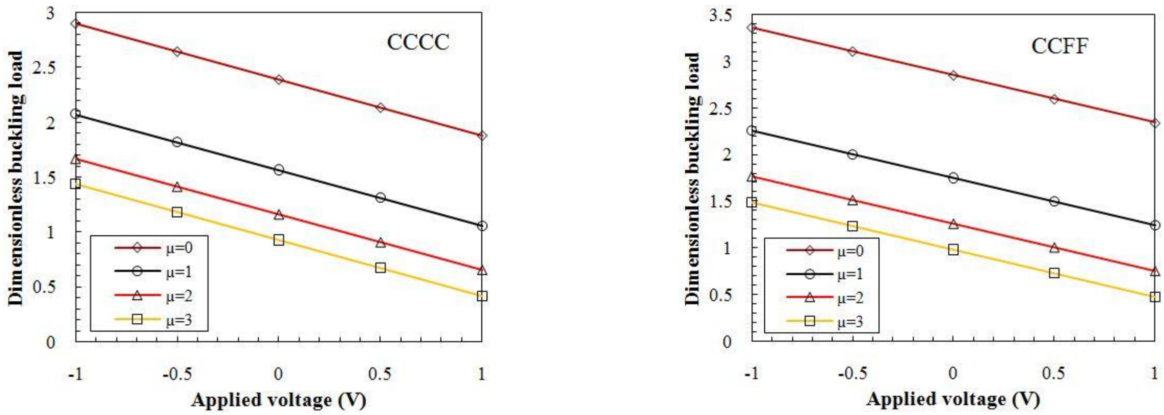

Fig. 5 Continued

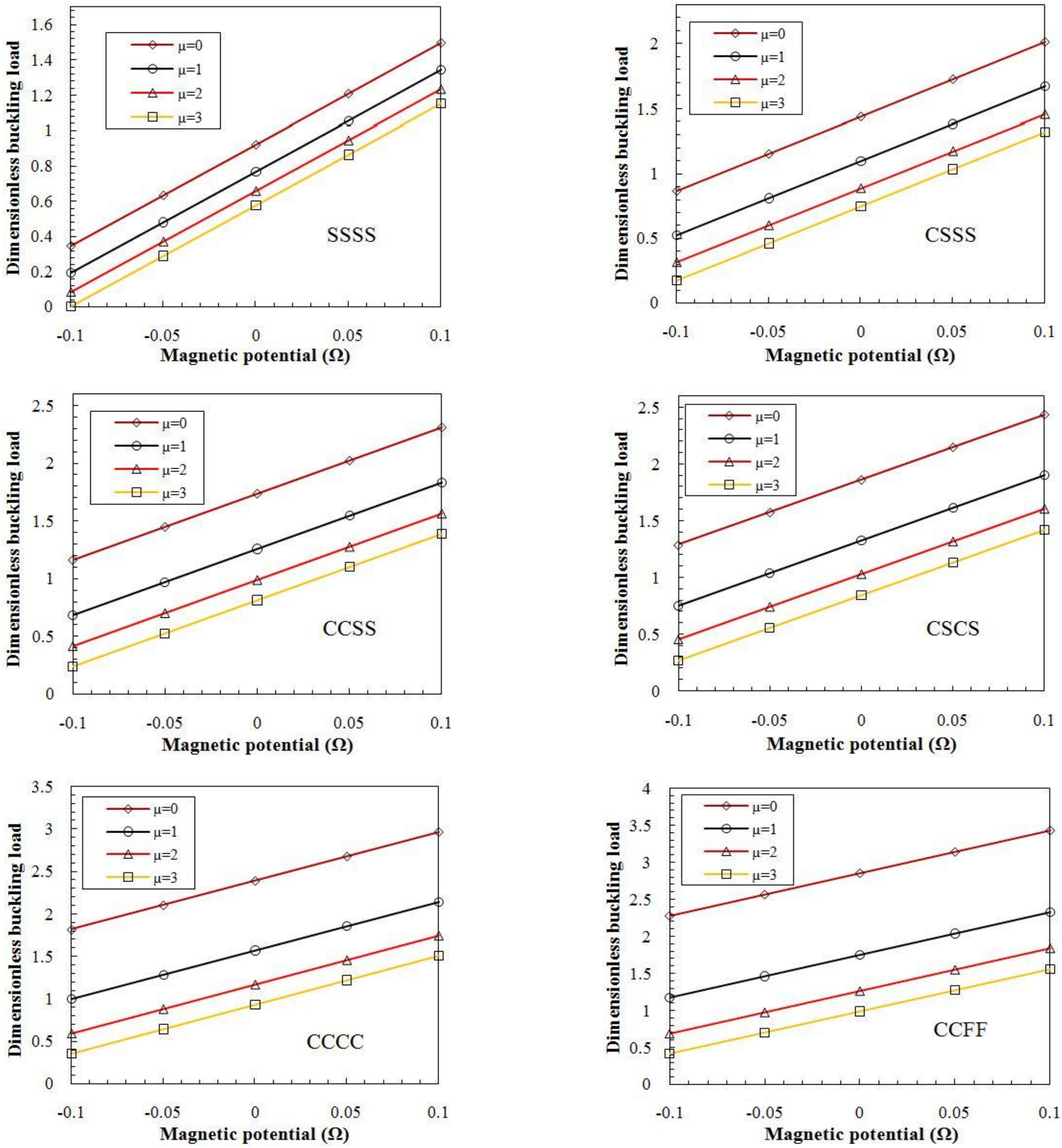

Fig. 6 Buckling load curves of the nanoplate versus magnetic potential for various nonlocal parameters (a/h = 100, p = 1, V = 0)

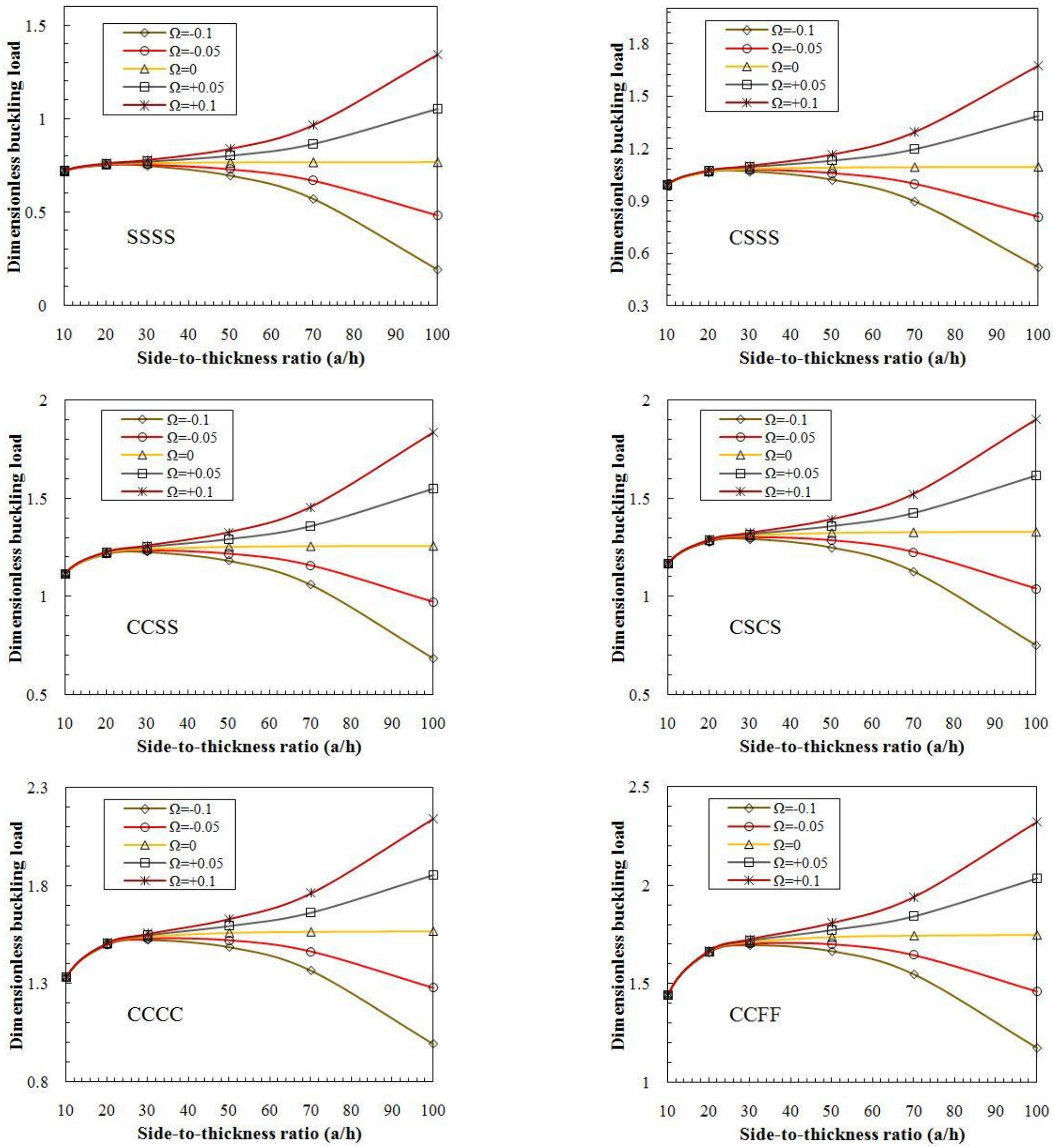

Fig. 7 Buckling load curves of the nanoplate versus side-to-thickness ratio for various magnetic potentials (μ = 1 nm^2, p = 1, V = 0×10^{-4})

larger buckling loads. Actually, the imposed positive/ negative magnetic potentials may produce the axial tensile and compressive forces. While electric field shows an opposite trend. It is also found that larger values of power-law index have no sensible influence on buckling loads. But, smaller values of power-law index show more significant effect on the variation of buckling loads. Also, it is assumed that the value of electric and magnetic potentials are equal to zero at the ends of the FG nanoplate. For the presented boundary conditions, a clamped-free MEE-FG nanoplate has the highest buckling loads, and the simply-supported one has the lowest buckling loads. For the MEE-FG nanoplate with intermediate boundary conditions, the results take the corresponding intermediate values.

Figs. 5 and 6 illustrate the variation of critical buckling loads of MEE-FG nanoplate versus electric voltage and magnetic potential, respectively for different nonlocal parameters when *a*/*h* = 100 and p = 1. It is deduced that buckling loads of nonlocal MEE-FG nanoplate are always smaller than that of local MEE-FG plate. Buckling loads decrease with the rise of the nonlocal parameter at a constant magnetic potential and electric voltage. Such phenomenon is owing to the fact that the small scale influence, which captures the mutual influence of all points in the region, may reduce the stiffness of the nanostructures. Also, nonlocal effect is more significant for a MEE-FG nanoplate with stronger supports at edges. Therefore, buckling loads of nanoplate with CCFF or CCCC boundary conditions are more affected by nonlocal parameter than other boundary conditions. It is also deduced that as the electric voltage and magnetic potential chnage from negative to positive values, the critical buckling loads respectively reduce and increase.

Depicted in Fig. 7 is the buckling load of the graded piezo-magnetic nanoplate with the change of length to thickness ratio (a/h) based on various magnetic potentials. There is no change in buckling load versus a/h when the magnetic potential is zero. Also, applying positive of negative magnetic potentials may increase or reduce the buckling load with respect to a/h.

5. Conclusions

Buckling characteristics of a quasi-3D piezo-magneric nanoplate were reported in the present article. The complete formulation and solution for the problem based on quasi-3D plate model was presented. There was no change in buckling load versus side to thickness ratio when the magnetic potential was zero. Also, applying positive of negative magnetic potentials led to increasing or reducing the buckling load with respect to side to thickness ratio. Also, it was reported that the buckling behavior of the nanoplate is sensitive to material gradient exponent. Another observation was that size effects due to nonlocality changed significantly the buckling behavior of piezo-magnetic nanoplate. Also, the dependency of buckling load to negative and positive voltages was clearly explained.

References

Ebrahimi, F. (2010), *Smart functionally graded plates*, Nova Science Publishers.

Ebrahimi, F. and Barati, M.R. (2016a), "A nonlocal higher-order shear deformation beam theory for vibration analysis of size-dependent functionally graded nanobeams", *Arab. J. Sci. Eng.*, **41**(5), 1679-1690.

Ebrahimi, F. and Barati, M.R. (2016b), "Dynamic modeling of a thermo–piezo-electrically actuated nanosize beam subjected to a magnetic field", *Appl. Phys. A*, **122**(4), 1-18.

Ebrahimi, F. and Barati, M.R. (2016c), "Buckling analysis of smart size-dependent higher order magneto-electro-thermo-elastic functionally graded nanosize beams", *J. Mech.*, 1-11.

Ebrahimi, F. and Barati, M.R. (2016d), "Vibration analysis of smart piezoelectrically actuated nanobeams subjected to magneto-electrical field in thermal environment", *J. Vib. Control*, 1077546316646239.

Ebrahimi, F. and Barati, M.R. (2016e), "An exact solution for buckling analysis of embedded piezoelectro-magnetically actuated nanoscale beams", *Adv. Nano Res., Int. J.*, **4**(2), 65-84.

Ebrahimi, F. and Barati, M.R. (2016f), "Buckling analysis of nonlocal third-order shear deformable functionally graded piezoelectric nanobeams embedded in elastic medium", *J. Brazil. Soc. Mech. Sci. Eng.*, 1-16.

Ebrahimi, F. and Barati, M.R. (2016g), "Electromechanical buckling behavior of smart piezoelectrically actuated higher-order size-dependent graded nanoscale beams in thermal environment", *Int. J. Smart Nano Mater.*, 1-22.

Ebrahimi, F. and Barati, M.R. (2016h), "Flexural wave propagation analysis of embedded s-fgm nanobeams under longitudinal magnetic field based on nonlocal strain gradient theory", *Arab. J. Sci. Eng.*, 1-12.

Ebrahimi, F. and Barati, M.R. (2016i), "Small scale effects on hygro-thermo-mechanical vibration of temperature dependent nonhomogeneous nanoscale beams", *Mech. Adv. Mater. Struct.*, **24**(11), 924-936.

Ebrahimi, F. and Barati, M.R. (2016j), "A unified formulation for dynamic analysis of nonlocal heterogeneous nanobeams in hygro-thermal environment", *Appl. Phys. A*, **122**(9), 792.

Ebrahimi, F. and Barati, M.R. (2016k), "A nonlocal higher-order refined magneto-electro-viscoelastic beam model for dynamic analysis of smart nanostructures", *Int. J. Eng. Sci.*, **107**, 183-196.

Ebrahimi, F. and Barati, M.R. (2018), "Stability analysis of functionally graded heterogeneous piezoelectric nanobeams based on nonlocal elasticity theory", *Adv. Nano Res., Int. J.*, **6**(2), 93-112.

Ebrahimi, F. and Dabbagh, A. (2018), "On wave dispersion characteristics of double-layered graphene sheets in thermal environments", *J. Electromag. Waves Appl.*, **32**(15), 1869-1888.

Ebrahimi, F., Sepiani, H.A. and Arani, A.G. (2011), *Progress in Analysis of functionally graded structures*, Nova Science Publishers.

Eringen, A.C. (1983), "On differential equations of nonlocal elasticity and solutions of screw dislocation and surface waves", *J. Appl. Phys.*, **54**(9), 4703-4710.

Hebali, H., Tounsi, A., Houari, M.S.A., Bessaim, A. and Bedia, E.A.A. (2014), "New quasi-3D hyperbolic shear deformation theory for the static and free vibration analysis of functionally graded plates", *ASCE J. Eng. Mech.*, **140**, 374-383.

Jia, X.L., Zhang, S.M., Yang, J. and Kitipornchai, S. (2013), "Pull-in instability of electrically actuated poly-SiGe graded Micro-beams", *Coupl. Syst. Mech., Int. J.*, **2**(3), 215-230.

Ke, L.L. and Wang, Y.S. (2014), "Free vibration of size-dependent magneto-electro-elastic nanobeams based on the nonlocal theory", *Physica E: Low-dimensional Syst. Nanostruct.*, 63, 52-61.

Li, Y.S., Cai, Z.Y. and Shi, S.Y. (2014), "Buckling and free vibration of magnetoelectroelastic nanoplate based on nonlocal theory", *Compos. Struct.*, **111**, 522-529.

Pan, E. and Han, F. (2005), "Exact solution for functionally graded and layered magneto-electro-elastic plates", *Int. J. Eng. Sci.*, 43(3), 321-339.

Ramirez, F., Heyliger, P.R. and Pan, E. (2006), "Discrete layer solution to free vibrations of functionally graded magneto-electro-elastic plates", *Mech. Adv. Mater. Struct.*, **13**(3), 249-266

Sobhy, M. (2015), "A comprehensive study on FGM nanoplates embedded in an elastic medium", *Compos. Struct.*, **134**, 966-980.

Tanaka, Y. (2018), "Active vibration compensator on moving vessel by hydraulic parallel mechanism", *Int. J. Hydromechatronics*, **1**(3), 350-359.

Tang, H., Li, L. and Hu, Y. (2019), "Coupling effect of thickness and shear deformation on size-dependent bending of micro/nano-scale porous beams", *Appl. Math. Model.*, **66**, 527-547.

Tounsi, A., Benguediab, S., Adda, B., Semmah, A. and Zidour, M. (2013), "Nonlocal effects on thermal buckling properties of double-walled carbon nanotubes", *Adv. Nano Res., Int. J.*, **1**(1), 1-11.

Wang, Z., Xie, Z. and Huang, W. (2018), "A pin-moment model of flexoelectric actuators", *Int. J. Hydromechatronics*, **1**(1), 72-90.

Wu, C.P., Chen, S.J. and Chiu, K.H. (2010), "Three-dimensional static behavior of functionally graded magneto-electro-elastic plates using the modified Pagano method", *Mech. Res. Commun.*, **37**(1), 54-60.

Zhang, Y.Q., Liu, G.R. and Xie, X.Y. (2005), “Free transverse vibrations of double-walled carbon nanotubes using a theory of nonlocal elasticity”, *Phys*. *Rev*., B 71, 195404.

Zenkour, A.M., Abouelregal, A.E., Alnefaie, K.A., Abu-Hamdeh, N.H. and Aifantis, E.C. (2014), “A refined nonlocal thermoelasticity theory for the vibration of nanobeams induced by ramp-type heating”, *Appl*. *Math*. *Comput*., **248**, 169-183.

CC